

Manufacture of ceramic bodies by using a mud waste from the TiO₂ pigment industry

M. Contreras^{1, a, *}, M.I. Martín^{2, b)}, M.J. Gázquez^{1, c)}, M. Romero^{2, d)} and J.P. Bolívar^{1, e)}

¹⁾ Department of Applied Physics, University of Huelva, Marine International Campus of Excellence (CEIMAR), 21071 Huelva, Spain

²⁾ Group of Glassy and Ceramic Materials, Department of Construction, Institute of Science Construction Eduardo Torroja (IETcc-CSIC), C/ Serrano Galvache 4, 28033 Madrid, Spain

^amanuel.contreras@dfa.uhu.es, ^bi.martin@csic.es, ^cmanuel.gazquez@dfa.uhu.es, ^dmromero@ietcc.csic.es, ^ebolivar@uhu.es

Keywords: Ceramic tile; NORM waste; ilmenite mud; red stoneware; valorisation.

Abstract

The main objective of this paper is focused in the use of a waste generated by the TiO₂ pigment industry, ilmenite mud (MUD), on the production of ceramic bodies. These ceramic bodies were produced from mixtures of a commercial red stoneware mixture (RSM) with different concentrations of mud (3, 5, 7, 10, 30 and 50 wt.%). The samples were sintered to simulate a fast-firing process. The sintering behaviour of the fired samples was evaluated by linear shrinkage, means of water absorption, apparent porosity and bulk density. Both green powder and fired samples were characterised by means of X-ray diffraction (XRD), differential scanning calorimetry (DSC/TG), field emission scanning electron microscopy (FESEM) and bending strength measurements. Moreover, the activity concentrations of radionuclides were measured by high-resolution low-background gamma spectrometry, because this mud is a NORM (Naturally Occurring Radioactive Material) waste. Finally, the TCLP leaching test (Toxicity Characteristic Leaching Procedure, USEPA) was performed to assess the risks of use tiles from an environmental perspective. The results demonstrated that MUD can be successfully valorised in the manufacture of red stoneware ceramic bodies with similar or even better technological properties than commercial materials used currently.

1. Introduction

Conversion of wastes into valuable materials (i.e. valorisation) is emerging as a strong trend because the growing awareness of the need for protection of health and environment. In this sense, the recovery of wastes currently generated in most industrial processes is the subject of a thorough investigation [1]. Wastes valorisation in building materials as secondary raw materials could allay the health and environment problems associated with both the depletion of natural resources and the disposal of industrial wastes [2], although the economic benefits accruing from waste recycling must not be ignored [3].

This work is focused on the recycling of waste -ilmenite mud (MUD) -generated by the TiO₂ pigment industry via sulphate, using concentrate sulphuric acid (80-95%) [4]. Around 30,000 tons per year of mud are generated without any use and it is disposed of in a waste repository [5]. Moreover, the natural radionuclides content is 100 times higher in relation to a typical soil, being classified as a NORM (Naturally Occurring Radioactive Material) industry presenting enhanced levels of radionuclides from the U and Th series [6]. A possible environmental solution to the disposal of a wide range of solid wastes could be their incorporation into ceramics [7]. The prospective benefits include immobilising of some heavy metals and radionuclides in the final

matrix, oxidising organic matter and destroying any pathogens during the firing process, based on the results of several full- or bench-scale studies [8]. Some publications study the possibility of recycling MUD in ceramics [9, 10].

The main objective of this work was to analyse the option of producing red stoneware (RNM) ceramics adding different ilmenite mud proportions and compare it with a standard commercial ceramic, studying its technological properties and the environmental implications.

2. Materials and methods

2.1. Materials and sample preparation. MUD was dried at 110°C for 48 hours until constant weight, and then grounded and sieved to a particle size >160 µm. According previous studies [11], MUD shows a high content of TiO₂, SiO₂, Al₂O₃ and iron oxide concentration (given as Fe₂O₃≈10%) similar to the RSM (natural clay: Fe₂O₃>7%) [4]. Mixtures of RSM (100/0) and different proportions of MUD (3 - 50%, code 97/3, 95/5, 93/7, 90/10, 70/30 and 50/50 respectively) were fired at 1150°C for eight minutes following the fast-firing process recommended by the red stoneware supplier (Tierra Atomizada, S.A.). The mixtures were moistened by spraying with distilled water (6 wt. %) and then shaped by uniaxial pressing (Nannetti S hydraulic press) at 40 MPa in a steel die, to obtain tiles measuring 50 x 50 x 5 mm.

2.2. Characterisation techniques. The mineralogy was performed by X-ray diffraction (XRD) which applied the method of dust lost. This method radiate with X-ray the sample formed by a multitude of crystals placed randomly in all directions as possible. It has been used a Bruker diffractometer (model D8 Advance), using Cu Kα radiation excited by a current of 30 mA and a voltage of 40 kV filtered with a sheet of nickel (monochromator) to eliminate the Kβ copper, allowing only the step of Kα radiation of wavelength known. Data were recorded in the 5-70° 2θ range (step size 0.019736° and 0.5 s counting time for each step). The measurement of trace elements and major elements was performed by inductively coupled plasma mass spectrometry (ICP-MS), using an HP branded computer model HP4500[®] and by inductively coupled plasma optical emissions spectrometer (ICP-OES) using a Jobin Yvon ULTIMA 2. Both systems were previously calibrated with the appropriate standards. Moreover, the microstructure of tiles was examined by field emission scanning electron microscopy (FESEM) (HITACHI model S-4800) operating at 20 kV. SEM specimens were polished with 6, 3 and 1 µm diamond pastes after grinding with silicon carbide paper and water and subsequently Au-Pd coated in a Balzers SCD 050 sputter. Finally, the thermal behaviour were evaluated by differential scanning calorimetry (DSC) and thermogravimetric analysis (TGA) (SETARAM model Labsys) on powder samples (size particle = 80-100 µm). DSC/TGA scans were performed between 25°C and 1450°C at 50°C/min in flowing air, platinum crucibles and calcined Al₂O₃ as reference material. The DSC/TG curves were normalised regarding the sample weight.

2.3. Technological characterisation. The sintering behaviour was evaluated on the basis of water absorption, apparent porosity and bulk density. The water absorption was measured according to EN ISO 10545-3 [12]. The water absorption coefficient, E (dry wt.%), was calculated by the equation:

$$E = [(m_2 - m_1)/m_1] \times 100 \quad (1)$$

where m_2 (g) is the mass of wet specimen and m_1 (g) is the mass of dry specimen. The apparent porosity and the bulk density were measured according to ASTM C373-88 [13], which involves drying the test specimens to constant mass (D). After impregnation, the mass (S) of each specimen while suspended in water and their saturated mass (M) was determined. The apparent porosity, P (%), expresses the relationship of the volume of open pores with the exterior volume of the specimen and is calculated as follows:

$$P = [(M - D)/(\rho \cdot V)] \times 100 \quad (2)$$

where V (cm^3) is the exterior volume ($V = M - S$) and ρ is the density of the water 1 g cm^{-3} . The bulk density, B (g cm^{-3}), of a specimen is the quotient of its dry mass divided by the exterior volume, including pores:

$$B = D/V \quad (3)$$

And the linear shrinkage, LS (%), calculated by the equation:

$$LS = (L_i - L_f) \times 100/L_i \quad (4)$$

where L_i (mm) is the specimen length without firing and L_f (mm) is the specimen length after firing. The bending strength, BS (MPa), was measured according to EN 843-1 [14] in an electronic universal tester (Servosis model ME-402/01) by a three-point loading test with a span of 32 mm and a crosshead speed of 1 mm/min.

All the test described in this section were carried out on ten representative specimens

2.4. Environmental implications. The activity concentrations of radionuclides were measured by high-resolution low-background gamma spectrometry with high-purity germanium detectors (HPGe). In addition, the concentrations of both Th-, U-isotopes and ^{210}Po were determined by the alpha spectrometry technique with ion-implanted Si detectors (PIPS detectors) [15]. Finally, to assess the risks of the use of a waste, the TCLP leaching test (Toxicity Characteristic Leaching Procedure, USEPA) was carried out [16]. The pollutant concentrations in the leaching dissolutions obtained from the mobility tests were analysed by ICP-OES and ICP-MS. In addition, the concentrations of different radionuclides contained in the leaching dissolutions were analysed by both alpha spectrometry techniques.

3. Results and discussion

3.1. Physico-chemical characterisation

3.1.1. Mineralogy. According previous works [11,17], the MUD showed several major mineral species such as ilmenite (FeTiO_3), rutile (TiO_2) anatase (TiO_2) and Fe-sulfates ($\text{FeSO}_4 \cdot x\text{H}_2\text{O}$ and $\text{Fe}_2(\text{SO}_4)_3$), and other minor mineral phases such as zircon (ZrSiO_4), quartz (SiO_2) and Fe and Ti oxides ($\text{Fe}_3\text{Ti}_3\text{O}_{10}$). On the other hand, the RSM showed as main mineral kaolinite ($\text{Al}_2\text{Si}_2\text{O}_5(\text{OH})_4$) and illite ($\text{KAl}_2\text{Si}_4\text{O}_{10}(\text{OH})_2$), with traces of quartz (SiO_2), anorthite ($\text{CaAl}_2\text{Si}_2\text{O}_8$), rutile (TiO_2) and hematite (Fe_2O_3) [18-20].

Figure 1 shows the diffraction patterns of samples after the firing process at 1150°C . The peaks associated with clay minerals (kaolinite and illite) are not detected because of the destruction of their crystalline structure between $450-900^\circ\text{C}$. At 1000°C the feldspar components (anorthite) undergo melting and form liquid phases [18]. In our case the potassium oxide released by illite decomposition could favour the agglomeration of the particles [19]. Ilmenite mud has an important content of iron and titanium oxides, which are known as nucleating agents that promote the crystallisation of mineral phases like anorthite [20]. Ilmenite, rutile and anorthite increased with MUD concentration, whereas quartz decreased in the ceramic body.

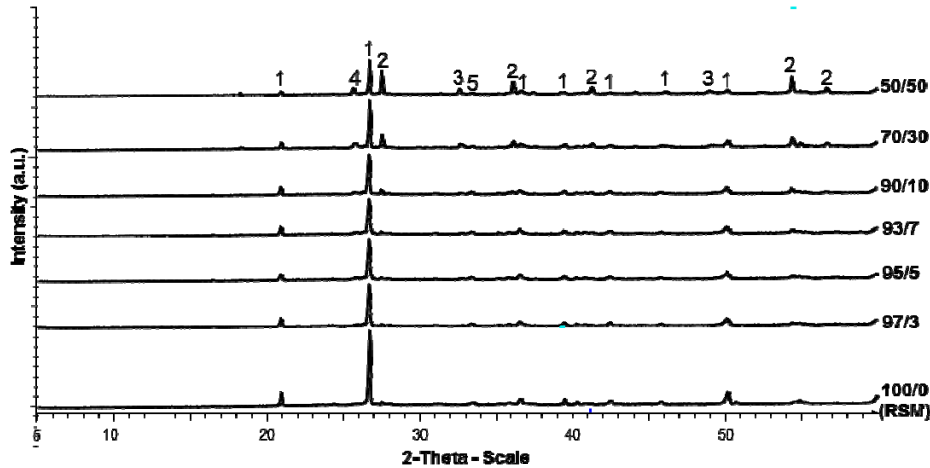


Figure 1. XRD patterns after the firing process. [1]: Quartz (SiO_2); [2]: Rutile (TiO_2); [3]: Ilmenite (FeTiO_3); [4]: Anorthite ($\text{CaAl}_2\text{Si}_2\text{O}_8$) and [5]: Ti and Fe oxides ($\text{Fe}_3\text{Ti}_3\text{O}_{10}$).

3.1.2. Chemical analysis. MUD shows a high content of TiO_2 (56 wt.%), SiO_2 (18 wt.%), Fe_2O_3 (10wt.%) and Al_2O_3 (5.1 wt.%) as expected [5] (Table 1). Moreover we found 2.60wt.% of SO_3 , due to MUD is produced by a sulphuric acid digestion. Also other elements as Zr (2.3wt.% of ZrO). On the other hand, RSM analysis reported SiO_2 (62 wt.%), Al_2O_3 (20 wt.%), Fe_2O_3 (7.4 wt.%) and K_2O (4.2 wt.%). Comparing both compositions, before and after firing, it is found that values were practically identical, only sulphur decreased from 2.60 to 0.05%, being released during the firing as sulphur oxide (SO_x) in MUD. The trace elements (As, Ba, Cr, Pb and Sr) were present at concentrations below 0.1% or 1000 mg kg^{-1} .

Table 1. Concentrations of major (wt. %) and trace (mg kg^{-1}) elements in the raw materials used in the manufacturing process of the tiles.

RSM/MUD	Major Elements								Trace Elements				
	Al_2O_3	CaO	Fe_2O_3	K_2O	SO_3	SiO_2	TiO_2	ZrO_2	As	Ba	Cr	Pb	Sr
MUD ¹⁾	5.12	1.11	10.37	1.29	2.60	18.43	56.43	2.30	< 3	480	901	282	130
0/100 (MUD ²⁾	5.95	1.54	10.32	1.27	0.05	18.23	57.73	2.47	13	785	500	281	135
RSM ¹⁾	19.94	2.10	7.39	4.20	0.06	62.00	1.67	0.32	10	568	69	39	108
100/0 (RSM ²⁾	21.30	2.09	9.04	4.25	0.06	58.88	1.67	0.32	9	601	71	58	116
90/10	20.73	1.98	9.66	4.12	0.06	52.94	6.62	0.47	< 3	594	129	68	113
50/50	13.78	1.68	10.30	2.94	0.15	39.01	28.22	1.34	< 3	737	319	182	129

¹⁾ Before firing process; ²⁾ After firing process

3.1.3. DSC/TGA. The thermal behaviour (Fig. 2a) of the RSM shows six areas of weight change. The first one at $\sim 100^\circ\text{C}$ corresponds to the endothermic evaporation of unbound water. The second area (between 200 and 500°C), is associated with the thermal decomposition of non-volatile organic compounds, the exothermic combustion of non-volatile organic matter and the endothermic volatilisation of lighter organic fragments. The third area at $\sim 600^\circ\text{C}$ is related to the thermal destabilisation of hydrated minerals and the release of crystallisation water. The fourth area $\sim 800^\circ\text{C}$ is associated with the decomposition of alkaline compounds. The fifth area $\sim 900^\circ\text{C}$ is associated with the decomposition of alkaline-earth carbonates and the release of carbon dioxide. Finally, an endothermic descent at high temperatures indicates the formation of a liquid phase mainly derived from the feldspar component and silica release [21]. Meanwhile, MUD shows five primary effects (Fig. 2b). The first one corresponds to the endothermic peak related to the slow and gradual loss of the chemically bound water of $\text{FeSO}_4 \cdot x\text{H}_2\text{O}$, which starts at $\sim 110^\circ\text{C}$. Moreover, the loss of moisture retained in the MUD sample is also included in this first effect at low temperature. The second area appears at $\sim 550\text{-}600^\circ\text{C}$ due to the loss weight produced by the thermal decomposition of FeSO_4 , associated with an endothermic reaction. The third area at $\sim 700^\circ\text{C}$ is associated with the decomposition of $\text{Fe}_2(\text{SO}_4)_3$ into Fe_2O_3 and the fourth area at $\sim 850^\circ\text{C}$

corresponds with the decomposition of calcium and potassium carbonate present in the ilmenite mud. Finally, an endothermic descent at higher temperatures indicates the formation of liquid phases [22].

DSC curves show that the thermal behaviours of the mixtures (Fig. 2c) are quite similar to the red stoneware (Fig. 2a), especially those that exhibit the greatest proportion of RSM (97/3, 95/5 and 93/7). In samples containing at least 10% in MUD appear new areas associated with MUD thermal behaviours. Figures 90/10, 70/30 and 50/50 show these new areas where both thermal behaviours converge. The first area at $\sim 100^\circ\text{C}$ (endothermic) evaporation of unbound water in RSM and the second at $\sim 110^\circ\text{C}$ (endothermic) due to the loss of bound water and decomposition of $\text{FeSO}_4 \cdot x\text{H}_2\text{O}$. Moreover, this same fact happens with the other different areas at $\sim 500\text{--}900^\circ\text{C}$ in which the thermal behaviour of both materials appears but less clear than in the previous case.

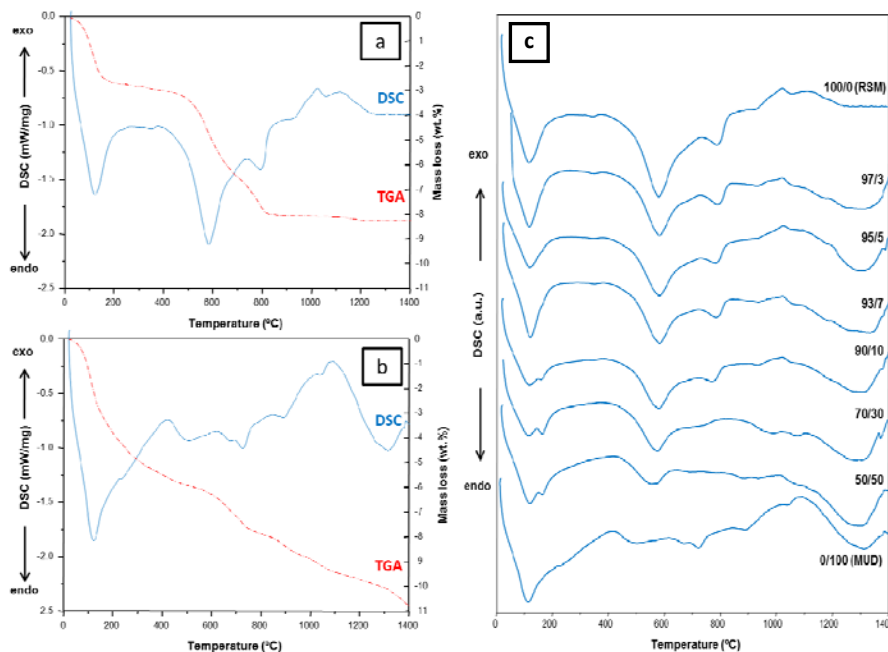


Figure 2. DSC/TGA curves (25-1450°C, 50°C/min) of a) RSM and b) MUD; and c) DSC curves (25-1450°C, 50°C/min) of 100/0 (RSM), 97/3, 95/5, 93/7, 90/10, 70/30, 50/50 and 0/100 (MUD).

3.1.4. Field emission scanning electron microscopy (FESEM). Ceramic bodies show good sintering behavior and a homogeneous grain and bond microstructure with coarse quartz particles held together by a finer matrix without internal defects (Figure 3).

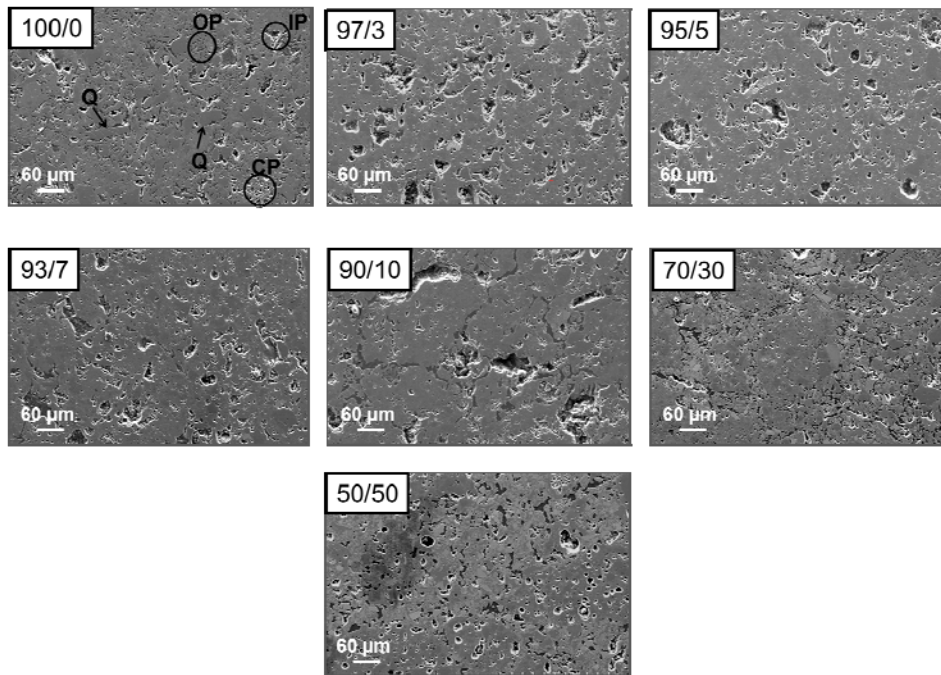


Figure 3. Secondary electron images (low magnification) on polished surfaces of fired tiles . Q: quartz; OP: open porosity; CP: close porosity and IP: interparticle porosity.

According Figure 4, RSM (100/0) is formed by open pores ($< 5 \mu\text{m}$) and close pores ($< 10 \mu\text{m}$). Also is observed pores with an irregular morphology at quartz and feldspar grain boundaries with the glassy matrix. After their allotropic transformation (573°C), quartz particles undergo pronounced shrinkage, increasing microscopic stresses. As the piece cools, the particles begin to debond from the matrix, giving rise to peripheral cracks [23]. MUD has a positive effect on the sinterization process, open porosity decreases in 97/3 and 95/5. Addition of MUD higher to 30% has increased significantly the volume of irregular intercommunicated channels.

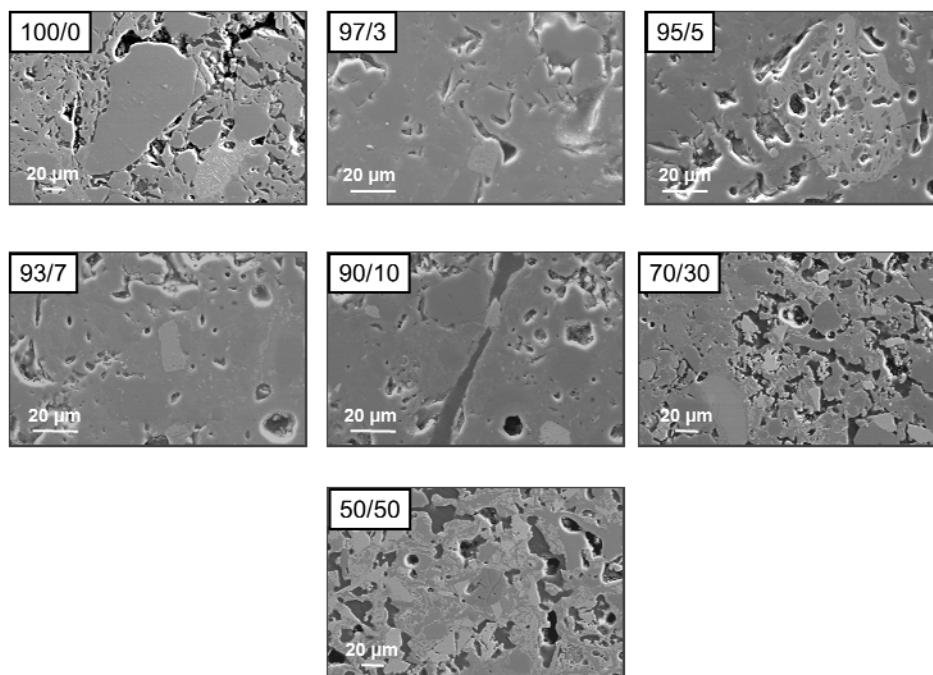


Fig. 4. Secondary electron images (high magnification) on polished surfaces of fired tiles.

3.2. Technological properties of fired tiles. The linear shrinkage (LS) increases with MUD addition (Table 2). Lower values ($< 7\%$) are advantageous because reduce cracking and volume

changes during firing. This result agrees the findings of Dondi et al. [9] who reported on the increase in linear shrinkage when MUD is introduced into carbonate-poor clay bodies. The apparent porosity generally increases with MUD concentration, related to the water absorption [12]. Moreover the water absorption (E) decreases with the addition of 3 and 5% of MUD (2.82 and 2.48 wt.%, respectively), facilitating the subsequent sintering and drying stages. On the other hand, the increase of irregular intercommunicated channels in samples 70/30 and 50/50, produce an increase in the water absorption, confirming the obtained results by SEM. This behavior is unexpected since an increase of porosity or water absorption usually corresponds to a decrease of firing shrinkage. This would imply an important effect of MUD on the porosity of the unfired bodies. The bulk density (B) increases with the addition of MUD up to 10% because the density of MUD is 3.7 g cm^{-3} . When the MUD content is higher than 30%, B decreases radically because of the increase in porosity. Regarding bending strength (BS), it can be seen that BS is inversely dependent on porosity. The bending strength (BS) with addition up to 10% of MUD shows higher values than reference tile (100/0), while addition of MUD higher of 10%, the values shows smaller than reference material. It is well known that BS in ceramic tiles is dependent on both the percentage of porosity but also on the size and shape of the pores. Thus, this result is likely due to the increase in the volume fraction of interconnecting open pores, which act as large fracture flaws reducing bending strength. The trend in water absorption and bending strength variation increasing MUD content disagree with the results found in studies on the re-use of MUD in brickmaking [9]. However, one must consider the processing method used for shaping the green bodies, which is different in each of the studies. Thus, bricks were conformed by plastic extrusion whereas green tiles were shaped by uniaxial pressing.

Table 2. Linear shrinkage and technological properties of fired tiles results show average values of 10 measurements.

RSM/MUD	Linear shrinkage	Apparent porosity	Water absorption	Bulk density	Bending strength
	LS (%)	P (%)	E (wt.%)	B (g cm^{-3})	BS (MPa)
100/0 (RSM)	3.8 ± 0.1	12.5 ± 0.7	5.30 ± 0.06	2.36 ± 0.02	35.1 ± 0.9
97/3	5.6 ± 0.1	6.71 ± 0.3	2.82 ± 0.05	2.38 ± 0.04	41.1 ± 0.8
95/5	6.0 ± 0.1	5.98 ± 0.2	2.48 ± 0.03	2.42 ± 0.05	40.2 ± 0.8
93/7	6.0 ± 0.1	10.0 ± 0.5	4.18 ± 0.04	2.40 ± 0.03	37.5 ± 0.7
90/10	6.4 ± 0.2	12.0 ± 0.7	4.72 ± 0.06	2.55 ± 0.03	36.5 ± 0.7
70/30	6.3 ± 0.1	19.8 ± 0.8	9.02 ± 0.10	2.22 ± 0.02	33.2 ± 0.8
50/50	6.6 ± 0.1	20.9 ± 0.9	9.18 ± 0.12	2.27 ± 0.05	30.8 ± 0.9

In accordance with the European Standard EN 14411 [24] ceramic tiles with water absorption coefficient (E) in the interval $0.5\% < E \leq 3\%$ and BS upper the minimum value of 30 MPa required in standard belong to the BI_b group (samples 97/3 and 95/5). Samples 93/7 and 90/10 are greater than 22 MPa, which is the minimum value and with $3\% < E \leq 6\%$ belong to the BII_a group and those with $6\% < E \leq 10\%$ and the minimum bending strength value of 18 MPa required belong to the BII_b group. The low values of water absorption and apparent porosity would make these tiles resistant to freeze-thaw cycles and stain resistant.

3.3. Environmental study

3.3.1. Radiological and radioactive characterisation. MUD is a NORM waste with an activity concentrations for ^{226}Ra and ^{228}Ra , around 400 and 1000 Bq kg^{-1} respectively (Table 3), higher than the average worldwide values for undisturbed soils (25 Bq kg^{-1} of ^{238}U and ^{232}Th in secular equilibrium with their daughters) [25]. The activity concentration in the mixtures increased with mud content, besides ^{40}K was constant in all samples. According the influence of the sintering process on the raw materials activity, no effects are appreciated, the activity concentration are quite similar after and before the firing process. Only ^{210}Po was drastically reduced during the firing process (from 300 to 70 Bq kg^{-1}), because of the high volatility of ^{210}Po above 200 °C [26].

In order to evaluate this waste as building material, the EU has proposed reference values for the natural radionuclide concentrations in building materials [27], defining an external risk index (I), also called activity concentration index, according to the following equation:

$$I = \frac{C^{226}Ra}{300 \text{ Bq / kg}} + \frac{C^{232}Th}{200 \text{ Bq / kg}} + \frac{C^{40}K}{3000 \text{ Bq / kg}} \quad (5)$$

where $C^{226}Ra$, $C^{232}Th$, and $C^{40}K$ are the activity concentrations for ^{226}Ra , ^{232}Th , and ^{40}K , respectively, expressed in $Bq \text{ kg}^{-1}$.

Table 3. Concentration in $Bq \text{ kg}^{-1}$ of each ceramics tile obtained and external risk rate “I”.

RSM/MUD	^{238}U	^{226}Ra	^{210}Po	^{232}Th	^{228}Ra	^{228}Th	^{40}K	“I”
RSM	39 ± 2	39 ± 3	37 ± 1	58 ± 3	54 ± 6	63 ± 7	832 ± 45	-
100/0 (RSM)	35 ± 2	50 ± 1	39 ± 2	60 ± 2	61 ± 2	56 ± 2	1104 ± 16	0.84
97-3	37 ± 2	55 ± 1	34 ± 2	62 ± 2	97 ± 3	84 ± 2	1154 ± 15	1.05
95-5	44 ± 2	72 ± 2	40 ± 2	59 ± 2	127 ± 4	108 ± 3	1182 ± 18	1.27
93-7	40 ± 2	79 ± 2	43 ± 4	59 ± 4	141 ± 5	118 ± 4	1158 ± 23	1.35
90-10	37 ± 2	75 ± 2	41 ± 2	63 ± 5	139 ± 5	112 ± 4	1124 ± 24	1.31
0/100 (MUD)	31 ± 1	457 ± 19	71 ± 4	78 ± 3	1158 ± 48	1112 ± 46	477 ± 30	7.47
MUD	34 ± 2	335 ± 15	300 ± 19	72 ± 4	952 ± 43	956 ± 43	428 ± 43	-

The index should not exceed the value of six ($I \leq 6$) for superficial materials, e.g. tiles, boards, etc., to ensure the external dose received by occupants does not exceed the reference value of 1 mSv year^{-1} [6]. Table 3 shows that index I is fairly lower than six for all analysed materials. This renders mud a suitable material for use in the ceramic industry in comparison with other additives [25-27].

3.3.2. Leaching test. According to TCLP test (Tables 4 and 5) the leached metals and radionuclides decrease while increasing the proportion of mud in the mixture. It is concluded that the firing process makes metal and radionuclides less leachable. On the other hand, S increases slightly as the proportion of ilmenite mud increases because of the sulphate breakdown during the firing process.

Table 4. Leachability concentrations of metals ($\mu\text{g L}^{-1}$) by TCLP test from the raw materials and tiles by ICP-OES.

RSM/MUD	Al	Ca	Fe	S	Si	Ti	Zn	As	Ba	Cr	Pb	Sr
100/0 (RSM)	8600	45400	314000	2000	29800	< 10	180	100	570	230	100	50
97/3	2000	14000	322000	3000	13700	< 10	88	40	400	200	300	60
95/5	1800	10400	312000	4000	5700	20	63	40	280	< 20	20	50
93/7	2100	17700	304000	5000	15500	< 10	122	60	310	240	150	40
90/10	2100	23100	300000	5000	15600	< 10	101	60	310	220	110	40
0/100 (MUD)	< 100	1200	40	< 1000	3700	70	40	< 30	40	< 20	< 10	< 10
Liquid1	< 100	< 100	20	< 1000	1300	< 10	10	< 30	< 20	< 20	< 10	< 10
U.S. EPA	-	-	-	-	-	-	25000	5000	1000000	5000	5000	-

Liquid 1 are the fluid extractant used in the TCLP test. The metals concentrations in the leachates have been subtracted the concentration of liquid 1

The concentrations of U-isotopes are of the same order of magnitude as typical ones in continental waters (Table 5), and for Th-isotopes they are one to two orders of magnitude higher, but we can ensure that their potential radiological impact is negligible [28]. On the other hand, the ^{210}Po increases slightly as the proportion of ilmenite mud increases. The data indicate that the metal and radionuclides concentrations are fairly below the ecotoxicity limits, clearly lower than the limits imposed by US EPA [29].

Table 5. Average radionuclides concentration (mBq L⁻¹) inleaching samples analyzed by alpha spectrometry

RSM/MUD	²³⁸ U	²³⁴ U	²³² Th	²³⁰ Th	²¹⁰ Po
100/0 (RSM)	13 ± 2	20 ± 3	37 ± 9	121 ± 17	16 ± 3
97/3	10 ± 2	10 ± 2	18 ± 6	54 ± 10	12 ± 2
95/5	4.8 ± 1.4	6.3 ± 1.7	33 ± 11	75 ± 17	10 ± 2
93/7	6.3 ± 1.4	5.1 ± 1.2	11 ± 4	24 ± 6	11 ± 3
90/10	6.4 ± 1.4	6.4 ± 1.4	5.1 ± 1.6	8.0 ± 2.0	5.5 ± 0.8
0/100 (MUD)	1.9 ± 0.8	1.4 ± 0.7	28 ± 11	91 ± 19	8.9 ± 1.9
Liquid 1	3.9 ± 1.4	8.3 ± 2.1	4.6 ± 2.6	8.0 ± 3.5	11 ± 2

Liquid 1 are the fluid extractant used in the TCLP test. The activity concentrations in the leachates have been subtracted the activity of liquid 1

4. Conclusions

The present work has demonstrated that MUD, waste coming from TiO₂ industry, can be successfully used in the manufacture of red stoneware ceramic. XRD analysis showed that, ilmenite, rutile and anorthite increased in the fired tiles with MUD concentration, whereas quartz decreased in the ceramic body. SEM analysis showed that composition with less than 10% of MUD has a finer fracture surface with fewer defects compared with reference (100/0). Leaching tests showed the mobility of metals and radionuclides in the several mixtures is similar to that of the reference tile.

The technological properties are comparable, or even better, than a commercial sample. The addition of 3-5% has a beneficial role as an agent of the sintering processes, decreasing both apparent porosity and water absorption, which facilitates the drying stage and improves the resistance to cycles of freeze-thaw and to stains thanks to the decrease in water absorption. Tiles can be classified into the following groups: samples with 3-5% of MUD belong to the BIb group with a 0.5% < E ≤ 3% and a minimum value BS of 30 MPa; tiles with 7-10% belong to the BIIa group, with 3% < E ≤ 6% and a minimum BS of 22 MPa. Additions of 30-50% classified into the BIIb group, with 6% < E ≤ 10% and a minimum BS of 18 MPa. In all cases, the tiles produced from ilmenite mud clearly exceed bending strength values required in the corresponding groups.

We think that effectively the use of ilmenite mud like additive in ceramic manufacturing could be the best potential application of this waste since its technological properties are significantly improved, and therefore this commercial application could consume all the ilmenite mud production due to the high amount of ceramic produced in worldwide.

Acknowledgements

PhD.s M. Contreras expresses her gratitude for the contract by The Fellowship Training Program of the University Teaching Staff; reference AP2010-2746, financed by the Spanish Ministry of Education, Culture and Sport (MECD) and by National Institution of Higher Education, Science, Technology and Innovation of the Republic of Ecuador – (SENESCYT for its acronym in Spanish), Prometeo Project. Dr. M.I. Martín expresses her gratitude for the contract JAE-Doc_08-00032 to the Spanish National Research Council (CSIC), co-financed by the European Social Fund Operational Programme 2007–2013 Adaptability and Employment Multiregional. This is a publication No. 92 from CEIMAR Publication Series.

References

- [1] Y. Liu, C. Lin, Y. Wu, Characterization of red mud derived of from a combined Bayer process and bauxite calcination method, *J. Hazard. Mater.* 146 (2007) 255–261.

- [2] M. Romero, A. Andrés, R. Alonso, J. Viguri, J.M. Rincón, Sintering behaviour of ceramic bodies from contaminated marine sediments, *Ceram. Int.* 34 (2008) 1917–1924.
- [3] N. Quijorna, A. Coza, A. Andresa, C. Cheeseman, Recycling of Waelz slag and waste foundry sand in red clay bricks, *Res. Con. Rec.* 65 (2012) 1-10.
- [4] M.J. Gázquez, J.P. Bolívar, R. García-Tenorio, F. Vaca, Physicochemical characterization of raw materials and co-products from the titanium dioxide industry, *J. Hazard. Mater.* 166 (2009) 1429–1440.
- [5] M.J. Gázquez, J. Mantero, J.P. Bolívar, Physico-chemical and radioactive characterization of TiO₂ undissolved mud for its valorization, *J. Hazard. Mater.* 191 (2011) 269–276.
- [6] UNSCEAR: Sources, effects and risks of ionizing radiation. Report to the General Assembly, with annexes. United Nations, New York, 1988.
- [7] L. Pérez-Villarejo, D. Eliche-Quesada, F. J. Iglesias-Godino, C. Martínez-García, F. A. Corpas-Iglesias, Recycling of ash from biomass incinerator in clay matrix to produce ceramic bricks. *J. Environ. Manage.* 95 (2012) S349-S354.
- [8] M.J. Gázquez, Characterization and recovery of waste generated in the industry for the production of titanium dioxide (Caracterización y valorización de residuos generados en la industria de producción de dióxido de titanio). University of Huelva. 2010.
- [9] M. Dondi, C. Zanelli, M. Raimondo, G. Guarini, D. Dalle Fabbriche, A. Agostini, Recycling titania slag insoluble residue (“Tionite”) in clay bricks. *Ceram. Int.*, 36 (2010) 2461-2467.
- [10] W. Hajjaji, G. Costa, C. Zanelli, M.J. Ribeiro, M.P. Seabra, M. Dondi, J.A. Labrincha, An overview of using solid wastes for pigment industry. *J. Am. Ceram. Soc.*, 32 (2012) 753-764.
- [11] M. Contreras, M.J. Gázquez, I. García-Díaz, F.J. Alguacil, F.A. López, J.P. Bolívar, Valorization of ilmenite mud waste for the manufacturing of Sulfur polymer cements, *J. Environ. Manage.* 128 (2013) 625-630.
- [12] ISO 10545-3:1997, Ceramic tiles. Part 3: Determination of water absorption, apparent porosity, apparent relative density and bulk density.
- [13] ASTM C373-88:1999, Standard test method for water adsorption, bulk density, apparent porosity and apparent specific gravity of fired whiteware products.
- [14] EN 843-1:2006, Advanced technical ceramics. Monolithic ceramics. Mechanical properties at room temperature. Part. I: Determination of flexural strength.
- [15] R.L. Lozano, J.P. Bolívar, E.G. San Miguel, R. García-Tenorio, M.J. Gázquez, An accurate method to measure alpha-emitting natural radionuclides in atmospheric filters: application in two NORM industries, *Nucl. Instrum. Meth. A.* 659 (2011) 557-568.
- [16] U.S. EPA, Test Methods for Evaluating Solid Waste Physical Chemical Methods, SW-846, U.S. Environmental Protection Agency, Washington, DC, (1997).
- [17] T. Chernet, Applied mineralogical studies on Australian sand ilmenite concentrate with special reference to its behaviour in the sulphate process, *Min. Eng.* 12 (1999) 485-495.

- [18] J. Martín-Márquez, J.Ma. Rincón, M. Romero, Effect of microstructure on mechanical properties of porcelain stoneware, *J. Am. Ceram. Soc.* 30 (2010) 3063–3069.
- [19] J. Martín-Márquez, J.Ma. Rincón, M. Romero, Effect of firing temperature on sintering of porcelain stoneware tiles, *Ceram. Int.* 34 (2008) 1867–1873.
- [20] J. Martín-Márquez, A.G. De la Torre, M.A.G.; Aranda, J.Ma. Rincón, M. Romero, Evolution with temperature of crystalline and amorphous phases in porcelain stoneware, *J. Am. Ceram. Soc.* 92 (2009) 229–34.
- [21] L.A. Pérez-Maqueda, V. Balek, J. Poyato, J.L. J. Pérez-Rodríguez, Šubrt, I.M. Bountsewa, I.N. Beckman, Z. Málek, Study of natural and ion exchanged vermiculite by emanation thermal analysis, TG, DTA AND XRD, *J. Therm. Anal. Calorim.* 71 (2003) 715–726.
- [22] S.M. Pérez-Moreno, M.J. Gázquez, A.G. Barneto, J.P. Bolívar, Thermal characterization of new fire insulating materials obtained from industrial inorganic wastes from TiO₂ industry, *Thermochim. Acta.* 552 (2013) 114-122.
- [23] A. De Noni, D. Hotza, V. Cantavella, E. Sanchez. Effect of quartz particle size on the mechanical behaviour of porcelain tile subjected to different cooling rates. *J.Eur. Ceram. Soc.* 29 (2009) 1039–1046.
- [24] EN 14411:2003, Ceramic tiles. Definitions, classifications, characteristics and marking.
- [25] Office European Commission Report on Radiological Protection- Principles concerning the natural radioactivity of building materials, Radiation Protection 112, for Official Publications of the European Communities, Luxembourg, 1999.
- [26] H. Mabuchi, On the volatility of some polonium, *J. Inorg. Nucl. Chem.* 25 (1963) 657-660.
- [27] K. Kovler, Radiological constraints of using building materials and industrial by-products, *Constr. Build. Mater.* 23 (2009) 246-253.
- [28] A. Hierro, J.E. Martín, M. Olías, C. García, J.P. Bolívar, Uranium behaviour during a tidal cycle in an estuarine system affected by acid mine drainage, *Chem. Geo.* 342 (2013) 110-118.
- [29] U.S. EPA, Test Methods for Evaluating Solid Waste - Physical Chemical Methods, SW-846, U.S. Environmental Protection Agency, Washington, DC, 1997.